Limitations on the measurement of unsteady flow velocities with a laser doppler velocimeter

W. K. George
Ordnance Research Laboratory, The Pennsylvania State University, U.S.A.

II.2-3 Limitations on the measurement of unsteady flow velocities with a laser doppler velocimeter

W. K. George
Ordnance Research Laboratory, The Pennsylvania State University, U.S.A.

Abstract

The utilization of the laser Doppler velocimeter in the measurement of unsteady fluid velocities has been limited by an inability to separate the Doppler ambiguity phase fluctuations from the velocity fluctuations.

The results of an exact theory for the effect of the ambiguity on the measurement of instantaneous fluctuating velocities are presented. The ambiguity is seen to arise from the fluctuating particle velocities, the finite particle transit time through the scattering volume, and mean velocity gradient across the volume; it is seen to be unavoidable regardless of the detection scheme utilized.

Criteria for minimization of the Doppler ambiguity are presented and conditions for meaningful measurements and data interpretation are established and illustrated with specific examples.

Nomenclature

$\underset{\sim}{a}$	initial position of scattering particle
e	exponential function
F, G,	random amplitudes of Doppler current; defined by Equations (16) and (17)
F^1_{11}	turbulence spectrum
g	random function which accounts for the presence or absence of a scattering particle
i	total current
i_{sp}	current generated by a single scattering particle
K	scattering wavenumber
k_*, m_*, n_*	defined by Equation (9)
k_o	defined by Equation (35)
R	defined by Equation (30)
R_D	pipe Reynolds number based on diameter
R_1	defined by Equation (39)
S	spectrum of Doppler current
$\underset{\sim}{u}$	Eulerian fluid velocity
u'	rms turbulent velocity
u_*	friction velocity
u_o	defined by Equation (6)

$\underset{\sim}{v}$	particle velocity
$\underset{\sim}{x}$	position of scattering particle
$\underset{\sim}{X}$	defined by Equation (11)
y'	distance from wall
α_o	frequency of unity turbulence to ambiguity spectrum
Δ	defined by Equation (18)
$\Delta\omega$	defined by Equation (22)
$\Delta\omega_G$	mean velocity gradient braodening
$\Delta\omega_L$	transit time broadening
$\Delta\omega_T$	broadening due to turbulent fluctuations within the scattering volume
$\Delta\omega_u$	broadening due to center frequency fluctuations
ϵ	rate of dissipation of turbulent energy per unit mass
λ	wavelength of incident radiation
μ	expected number of particles per unit volume
ν	kinematic viscosity
ϕ	random phase of Doppler current, defined by Equation (15)
σ_1, σ_2, σ_3	standard deviation of scattering volume
θ	scattering angle
ω	spectral frequency
$\bar{\omega}_o$	mean Doppler beat frequency

1. Introduction

In 1964, Yeh and Cummins successfully measured velocity profiles in a liquid by examining the frequency shift of monochromatic radiation scattered from particles suspended in the liquid. The scattered and unscattered radiation was heterodyned on a photocell producing an electrical signal at the difference frequency.

Since 1964 numerous investigators have attempted to apply the Laser Doppler Velocimeter to the measurement of unsteady fluid velocities. These attempts have been inhibited by the presence of random phase fluctuations (Doppler ambiguity) inherent in the scattering process which 'contaminate' the velocity signal.

The application of the Laser Doppler Velocimeter to the measurement of unsteady flow velocities has been the subject of extensive theoretical and experimental investigation by George (1971) and George and Lumley (1972).* This paper attempts to present their results and demonstrate their application to particular flow problems.

2. Representation of the Doppler Signal

The Doppler current generated at the photocell by a single scattering particle may be shown to be given by

$$i_{sp}(t) = I\, e^{-\left\{\frac{x^2}{2\sigma_1^2} + \frac{y^2}{2\sigma_2^2} + \frac{z^2}{2\sigma_3^2}\right\}} \cos \underset{\sim}{K} \cdot \underset{\sim}{x} \qquad (1)$$

*hereafter referred to as Reference I and II respectively.

where $(x, y, z) = \underset{\sim}{x}$ is the location of the particle with respect to the center of the scattering volume which has been chosen to be Gaussian with standard deviations σ_1, σ_2, σ_3 (see Figure 1). I depends on the intensity of the beams as well as the scattering cross-section of the particle. $\underset{\sim}{K}$ is defined as the scattering vector and the coordinate system is aligned so that $\underset{\sim}{K} = (K, o, o)$ where K is given by

$$K = \frac{4\pi}{\lambda} \sin \theta/2 \tag{2}$$

θ is the scattering angle and λ is the wavelength of the incident radiation.

The position of the particle may be expressed in terms of its initial position $\underset{\sim}{a}$ and velocity history $\underset{\sim}{v}(\underset{\sim}{a}, t)$ as

$$\underset{\sim}{x}(\underset{\sim}{a}, t) = \underset{\sim}{a} + \int_0^t \underset{\sim}{v}(\underset{\sim}{a}, t_1)\, dt_1 \tag{3}$$

Generally, $\underset{\sim}{a}$ is a random variable and $\underset{\sim}{v}(\underset{\sim}{a}, t)$ is taken as the material velocity of the fluid point initially at $\underset{\sim}{a}$. Substitution of Equation (3) into Equation (1) reveals that the phase of the Doppler current from a single particle is fixed by the initial position of the particle and the time dependence is determined by the particle velocity.

We may sum over all particles to obtain the total Doppler current,

$$i(t) = \sum_{n=1}^{N(t)} I_n\, e^{-\left[\frac{x_n^2}{2\sigma_1^2} + \frac{y_n^2}{2\sigma_2^2} + \frac{z_n^2}{2\sigma_3^2}\right]} \cos K x_n \tag{4}$$

where N(t) is the instantaneous number of scattering particles. Since the scattering volume is unbounded and, hence, N(t) infinite, it is more convenient to write

$$i(t) = \iiint i(t, \underset{\sim}{a})\, g(\underset{\sim}{a})\, d\underset{\sim}{a} \tag{5}$$

where $i(t, \underset{\sim}{a})$ is the current generated by the particle with initial position $\underset{\sim}{a}$ and $g(\underset{\sim}{a})$ is a delta function with random argument accounting for the presence or absence of a particle at a point.

3. The Effective Fluid Velocity

We define an "effective" velocimeter velocity as

$$\underset{\sim}{u}_o(t) = \frac{1}{\mu} \iiint \underset{\sim}{u}(\underset{\sim}{a}, t)\, g(\underset{\sim}{a})\, w\left[\underset{\sim}{x}(\underset{\sim}{a}, t)\right] d\underset{\sim}{a} \tag{6}$$

where μ is the expected number of particles per unit volume and $w[\underset{\sim}{x}(\underset{\sim}{a}, t)]$ weights the particle velocities by the amplitude of their signal at any instant. Using Equation (1) and normalizing to unit volume, we have

$$w\left[\underset{\sim}{x}\right] = \frac{1}{(2\pi)^{3/2}\, \sigma_1 \sigma_2 \sigma_3}\, e^{-\left[\frac{x^2}{2\sigma_1^2} + \frac{y^2}{2\sigma_2^2} + \frac{z^2}{2\sigma_3^2}\right]} \tag{7}$$

For a finite (off-on) scattering volume this definition of $u_o(t)$ is equivalent to

$$\underset{\sim}{u}_o(t) = \frac{1}{N} \sum_{n=o}^{N} \underset{\sim}{u}_n (\underset{\sim}{x}_n, t) \tag{8}$$

George and Lumley (1972) have shown that if the scattering volume is significantly smaller than the scale of the inhomogeneities of the turbulence, then $\underset{\sim}{u}_o(t)$ is the Eulerian (or flow) velocity at the center of the scattering volume to within the resolution of the scattering volume. Spectral attenuation at high wavenumbers is caused by the finite size of the scattering volume. In Figure (2), the wavenumber spectrum is plotted for several values of the cutoff wavenumbers of the scattering volume defined as

$$k_*,\ m_*,\ n_* = \left(\frac{1}{\sqrt{2}\sigma_1}, \frac{1}{\sqrt{2}\sigma_2}, \frac{1}{\sqrt{2}\sigma_3}\right) \tag{9}$$

It is easily seen that velocity variations of smaller spatial extent than the largest dimension of the scattering volume are significantly attenuated.

In flows with mean velocity gradients, particular attention must be paid to the restriction regarding the relative sizes of the scattering volume and flow inhomogeneities. Edwards et al. 1971 have shown that if the velocity profile has appreciable curvature within the scattering volume, the measured u_o will be higher than the velocity at the center of the scattering volume. This is of particular importance in capillary flows. The contamination of the measured turbulent velocities in the presence of a large mean velocity gradient also leads to a serious problem in the interpretation of the measurements. A criterion for reliable turbulence measurements in the presence of a mean velocity gradient may be taken as

$$\sigma \ll \frac{\bar{u}}{\nabla \bar{u}} \tag{10}$$

where $\bar{u}/|\nabla u|$ defines a characteristic length for the flow and σ is the dimension of the scattering volume in the direction of the maximum gradient.

4. The Spectrum of the Doppler Current

Using Equation (6) we may define an equivalent displacement field by

$$\underset{\sim}{X}(t) = \int_o^t \underset{\sim}{u}_o(t_1)\, dt_1 \tag{11}$$

The position of a particle may now be written as

$$\underset{\sim}{x}(t) = \underset{\sim}{a} + \underset{\sim}{X}(t) + \int_o^t \left[\underset{\sim}{u}(a,t_1) - \underset{\sim}{u}_o(t_1)\right] dt_1 \tag{12}$$

Using this in Equation (5) we may write the total Doppler current as

$$i(t) = F(t) \cos K\, X(t) + G(t) \sin K\, X(t) \tag{13}$$

or

$$i(t) = \left[F^2 + G^2\right]^{1/2} \cos\left[K\, X - \phi\right] \tag{14}$$

where

$$\phi = \tan^{-1} \frac{G}{F} \tag{15}$$

and where F and G are defined by

$$F(t) = \iiint e^{-\left[\frac{x^2}{2\sigma_1^2} + \frac{y^2}{2\sigma_2^2} + \frac{z^2}{2\sigma_3^2}\right]} \cos K\left[\underset{\sim}{a} + \Delta(\underset{\sim}{a}, t)\right] d\underset{\sim}{a} \qquad (16)$$

$$G(t) = -\iiint e^{-\left[\frac{x^2}{2\sigma_1^2} + \frac{y^2}{2\sigma_2^2} + \frac{z^2}{2\sigma_3^2}\right]} \sin K\left[\underset{\sim}{a} + \Delta(\underset{\sim}{a}, t)\right] d\underset{\sim}{a} \qquad (17)$$

We have defined a deviation function as

$$\Delta(\underset{\sim}{a}, t) = \int_0^t \left[u(\underset{\sim}{a}, t_1) - u_o(t_1)\right] dt_1 \qquad (18)$$

It is clear from the definitions that $\Delta(\underset{\sim}{a}, t)$ will reflect the presence of velocity variations within the scattering volume as well as the effect of a mean velocity gradient.

We are now in a position to evaluate the spectrum of the Doppler current by choosing appropriate statistics for the turbulence. By taking the probability density of the turbulent displacements to be Gaussian it may be shown that (cf. I, II)

$$S(\omega) = e^{-(\omega - \overline{\omega}_o)^2 / 2\left[\Delta\omega_u^2 + \Delta\omega^2\right]} + e^{-(\omega + \overline{\omega}_o)^2 / 2\left[\Delta\omega_u^2 + \Delta\omega^2\right]} \qquad (19)$$

where

$$\overline{\omega}_o = K\,\overline{u}_o \qquad (20)$$

and thus corresponds to the mean velocity;

$$\Delta\omega_u^2 = K^2\, u'^2 \qquad (21)$$

where u'^2 is the turbulent energy. $\Delta\omega$ represents an ambiguous Doppler broadening, or Doppler ambiguity, and may be shown to be given by

$$\Delta\omega^2 = \Delta\omega_L^2 + \Delta\omega_T^2 + \Delta\omega_G^2 \qquad (22)$$

where $\Delta\omega_L$ represents the effect of the finite transit time of particles through the beam, $\Delta\omega_T$ represents the effect of the displacement deviations across the volume, or equivalently, the velocity fluctuations within the volume; and $\Delta\omega_G$ represents the broadening due to the mean velocity gradient. From I and II we have

$$\Delta\omega_L = \overline{u}/\sqrt{2}\,\sigma_1 \qquad (23)$$

It is clear that $\sigma_1/\overline{u}$ is proportional to the transit time of a particle across the volume. Also from I and II, if we restrict ourselves to a small scattering volume (i.e. σ_1, σ_2, $\sigma_3 \sim \eta$ where η is the Kolmogorov microscale of the turbulence) and to small scattering angle ($\sin\theta/2 < 0.3$), we have

$$\Delta\omega_T = \sqrt{2/15}\, K\, \sigma_2\, (\epsilon/\nu)^{1/2} \qquad (24)$$

where ϵ is the rate of dissipation of turbulent energy per unit mass and ν is the kinematic viscosity. $(\epsilon/\nu)^{1/2}$ is the frequency characteristic of the turbulent fine structure; thus, $\Delta\omega_T$ increases linearly with the highest frequency of the turbulence and the largest dimension of the scattering volume. Finally, the mean velocity gradient broadening may be estimated by

$$\Delta\omega_G = K \frac{\partial \bar{u}}{\partial y} \sigma_2 \qquad (25)$$

and is seen to increase linearly with the mean velocity gradient and scattering volume size.

Doppler broadening is also caused by the Brownian motion of the scattering particles and the non-monochromaticity of the source; these are usually negligible and will be ignored here.

In a laminar flow with no significant mean velocity gradient, only $\Delta\omega_L$ survives and the resultant spectrum from Equation (19) is shown in Figure (3a). If the flow is turbulent, both $\Delta\omega_T$ and $\Delta\omega_u$ are also present and the spectrum would appear as in Figure (3b).

Some investigators have suggested that the root-mean-square turbulent energy is proportional to the width of the spectrum in turbulent flow minus the width of the spectrum in laminar flow. Clearly, because of the presence of $\Delta\omega_T$, this is not so.

A criterion for determination of the turbulent energy from the spectral width might be taken as

$$\Delta\omega << Ku' \qquad (26)$$

It should be noted that even when Equation (26) is satisfied, since the spectral width $\Delta\omega_u$ is in general determined by the second moment of the turbulent displacement field, care must be exercised in identifying $\Delta\omega_u$ with u', the root-mean-square velocity fluctuation (cf. I and II). Equation (21) is strictly true only when X(t) has a Gaussian distribution.

Before proceeding further, we will illustrate the relative magnitude of the Doppler ambiguity bandwidths in a typical flow situation--a turbulent pipe flow. In the core region we will estimate the relevant parameters as follows:

$\bar{u} \sim U$, $\partial\bar{u}/\partial y \sim 2^{u*}/D$ and $\epsilon \sim 4u_*^2U/D$ where U is the centerline velocity, u_* is the friction velocity, and D is the pipe diameter. Near the wall (viscous sublayer) we may estimate

$$\bar{u} = \left|\frac{\partial u}{\partial y}\right| y = \frac{u_*^2}{\nu} y, \qquad \epsilon = \frac{u_*^4}{4\nu}, \qquad \frac{\partial \bar{u}}{\partial y} = \frac{u_*^2}{\nu}$$

By substituting into Equations (22 - 25) we may estimate the Doppler broadening. The results are summarized in Table 1 where we have defined

$$R_D = \frac{\bar{u}D}{\nu}$$

Table 1

	Core	Wall Region
$\frac{\Delta\omega_L}{\overline{\omega}_o}$	$\frac{1}{\sqrt{2}K\sigma_1}$	$\frac{1}{\sqrt{2}\,K\sigma_1}$
$\frac{\Delta\omega_T}{\Delta\omega_L}$	$\frac{4}{\sqrt{15}}\,K\sigma_1\,(\frac{\sigma_1}{D})\,(\frac{\sigma_2}{\sigma_1})\,\frac{u_*}{u}\,R_D^{1/2}$	$\frac{1}{\sqrt{15}}\,K\sigma_1(\frac{\sigma_2}{\sigma_1})\,(\frac{\sigma_1}{y})$
$\frac{\Delta\omega_G}{\Delta\omega_T}$	$\sqrt{\frac{15}{2}}\,\frac{\sigma_1}{\sigma_2}\,R_D^{-1/2}$	$\sqrt{30}\,\frac{\sigma_1}{\sigma_2}$

We will compute these ratios for the particular case where

$R_D \sim 10^5$ $\qquad\qquad$ $\sigma_1 = 10\ \mu m$

$\frac{u_*}{U} \sim 0.04$ $\qquad\qquad$ $K = 2 \times 10^3\ mm^{-1}$

$\sin\theta/2 \sim 0.1$ $\qquad\qquad$ $D = 0.1\ m$

Using these we have

$$\frac{\sigma_1}{\sigma_2} \sim 0.1, \quad \frac{\sigma_1}{D} \sim 10^{-4}, \quad K\sigma_1 \sim 20, \quad \frac{\sigma_1 u_*}{\nu} \sim 0.4$$

Substituting into Table I, we obtain the values of Table II.

Table II

	Core Region	Wall Region (at $yu_*/\nu = 1$)
$\frac{\Delta\omega_L}{\overline{\omega}_o}$	3×10^{-2}	3×10^{-2}
$\frac{\Delta\omega_T}{\Delta\omega_L}$	2×10^{-1}	2×10^{1}
$\frac{\Delta\omega_G}{\Delta\omega_T}$	10^{-2}	0.5

For the parameters chosen, it is clear that in the core region the mean velocity gradient broadening is negligible; the transit time broadening is greater than the turbulent broadening by a factor of five.

Near the wall, however, the mean velocity gradient broadening and the turbulent broadening are nearly equal and are much greater than the transit time broadening. The ratio $\Delta\omega/\overline{\omega}_o$ is nearly unity rendering measurement impossible by the criterion of Equation (26) since $u'/\overline{u} \sim 0.3$. Also, since $\sigma_1 u_*/\nu \sim 0.4$, the criterion of Equation (10) is not satisfied.

From Equations (22 - 25) it is easy to show that an optimum volume size exists which minimizes the Doppler ambiguity bandwidth $\Delta\omega$. If there is no mean velocity gradient, the optimum size is attained when $\Delta\omega_L = \Delta\omega_T$, or when

$$\frac{u}{\sqrt{2}\sigma_1} = \sqrt{\frac{2}{15}}\ K\sigma_2 \left(\frac{\epsilon}{\nu}\right)^{1/2} \qquad (27)$$

For small scattering angle

$$\sigma_2 \simeq \frac{\sigma_1}{\sin\frac{\theta}{2}} \qquad (28)$$

Hence the optimum scattering volume size is given by

$$\sigma_1^2 = \frac{\sqrt{15}}{2}\ \bar{u}\ \frac{\sin\frac{\theta}{2}}{K\left(\frac{\epsilon}{\nu}\right)^{1/2}} \qquad (29)$$

Defining

$$R = \frac{2\pi\ \bar{u}}{\nu\ K} \qquad (30)$$

(to be consistent with I and II) and using the Kolmogorov microscale η defined by

$$\eta = \left(\frac{\nu^3}{\epsilon}\right)^{1/4} \qquad (31)$$

we obtain

$$\frac{\sigma_{1\,optimum}}{\eta} = 0.56\ \left(R \sin\frac{\theta}{2}\right)^{1/2} \qquad (32)$$

Applying this to the core region of the example above we find that the optimum volume size for this flow is

$$\sigma_1 \sim 20\mu m$$

or about double the value we chose in the example.

A similar optimization can be carried out in the wall region where here the goal is to reduce the mean velocity gradient and turbulent ambiguity while increasing the transit time ambiguity until the minimum value of $\Delta\omega$ is reached. In the example this clearly will involve a reduction in scattering volume size. In general, the same scattering volume will not be an optimum over the entire flow to be investigated.

5. The Measurement of Instantaneous Velocities

A typical detection device removes the amplitude information yielding a signal proportional only to frequency, say ω_1, where

$$\omega_1 = K\ u_o(t) - \dot{\phi}(t) \qquad (33)$$

From Equations (16) and (17), it is easily seen that F and G are random variables because of their dependence on a; hence, from Equation (15), ϕ is also random as is $\dot{\phi}(t)$. Thus the detector responds, not only to the velocity fluctuation $u_o(t)$, but also to the random phase fluctuations $\dot{\phi}(t)$.

Using the fact that F and G are nearly Gaussian if there is a sufficient number of scattering particles (say $\mu\ \sigma_1\ \sigma_2\ \sigma_3 > 10$), George and Lumley (I and II) were able to predict the statistics of $\dot{\phi}(t)$; in particular, the spectrum of $\dot{\phi}(t)$. The spectrum of $\dot{\phi}(t)$ at zero frequency was shown to have a value equal to the total Doppler bandwidth $\Delta\omega$. The spectrum was also shown to be almost flat to a frequency of about $\Delta\omega$ and to fall as inverse frequency thereafter. These predictions were confirmed by experiment.

Since the Doppler ambiguity fluctuations $\dot{\phi}$ have such a broad spectrum ($\Delta\omega$ is generally well above the highest frequency of the turbulence), the velocity signals, $u_o(t)$, are contaminated at all frequencies - the degree of contamination depending on the relative spectral heights of the turbulence and ambiguity spectra.

If we call the frequency at which the turbulence spectrum and the ambiguity spectrum intersect the cutoff frequency, α_o, then

$$F_{11}^{1}\left(\frac{\alpha_o}{\bar{u}}\right) = \bar{u}\,\frac{\Delta\omega}{K^2} \tag{34}$$

where $F_{11}^{1}(\alpha)$ is wavenumber spectrum of the turbulence and Taylor's hypothesis has been used to write the frequency explicitly. By defining the cutoff wavenumber k_o as

$$k_o = \frac{\alpha_o}{\bar{u}} \tag{35}$$

and nondimensionalizing by Kolmogorov variables ϵ and ν, we may write

$$\tilde{F}_{11}^{1}(\tilde{k}_o) = \frac{\bar{u}\,\Delta\omega}{K^2}\,\epsilon^{-1/4}\,\nu^{-5/4} \tag{36}$$

Using the R defined in Equation (30) and the definition of the Kolmogorov microscale η, we may write

$$\tilde{F}_{11}^{1}(\tilde{k}_o) = 2.53 \times 10^{-2}\,R^2\left[\frac{\Delta\omega\eta}{\bar{u}}\right] \tag{37}$$

Figure (4) shows a plot of Pao's spectrum for the turbulence $\tilde{F}_{11}^{1}(\tilde{k})$ along with plots of the Doppler ambiguity spectra for the particular case $\Delta\omega\eta/\bar{u} \approx \sqrt{2}$. The points of intersection of the curves determine the $\tilde{k}_o$ of Equation (37) and thus the limit of measurement.

If we again ignore mean velocity gradients and optimize the scattering volume as in Equation (32) to minimize $\Delta\omega$, we may use Equation (37) and Pao's spectrum to calculate the maximum wavenumber to which the spectrum can be measured. Under these conditions we may easily show that

$$\tilde{F}_{11}^{1}(\tilde{k}_o) = 4.27 \times 10^{-2}\,R_1^{3/2} \tag{38}$$

represents implicitely the maximum cutoff wavenumber where

$$R_1 = \frac{R}{\left(\sin\frac{\theta}{2}\right)^{1/3}} \tag{39}$$

A plot of this maximum wavenumber (wavenumber at which turbulence spectrum and ambiguity spectrum are equal under optimum conditions) is shown in Figure (5) as a function of R_1.

For the core region of the pipe flow considered above $R_1 = 6.75$. From Figure (5) the highest k_o that can be measured is $k_o \sim 0.2$. Thus the frequency at which the turbulence spectral height is equal to the height of the ambiguity is about one fifth of the frequency corresponding to the Kolmogorov microscale. Clearly, measurement in the dissipative range of the turbulence is impossible in this situation. A similar calculation can be performed near the wall where here the mean velocity gradient broadening must also be considered.

Since the Doppler ambiguity fluctuations are uncorrelated with the velocity fluctuations, a certain amount of subtraction can be carried out as shown in the data of Figure (6) taken from References I and II. Care must be exercised to ascertain that the turbulence has not been attenuated by the size of the sampling volume as described in Section (3). Figure (7) shows a plot of both the wavenumber of unity turbulence to ambiguity spectral heights and the wavenumber of half power attenuation. We have chosen $\sin \theta/2 = 0.145$ and have used the optimum scattering volume of Equation (32).

6. Two Point Velocity Correlation

If two point correlations are performed using two independent velocimeters with non-overlapping scattering volumes, the Doppler ambiguity fluctuations are uncorrelated and only the velocity correlation is obtained. Consequently two point velocity correlations are possible and are independent of the sources of Doppler broadening.

7. Summary and Conclusion

The Doppler ambiguity has been shown to provide a major limitation on the use of the laser Doppler velocimeter in unsteady flow measurement. The ambiguity arises primarily from the finite transit time through the scattering volume, the turbulent velocity fluctuations within the volume, and the mean velocity gradients across the volume.

It should be pointed out that the Doppler ambiguity is unavoidable in single point measurements regardless of the detection system used.

Acknowledgements

The author is grateful to Professor J. L. Lumley of The Pennsylvania State University for his contributions to this work and to the Ordnance Research Laboratory for their financial support.

Bibliography

Edwards, R. V., J. C. Angus, M. J. French, and J. W. Dunning, Jr. (1971), "Spectral Analysis of the Signal from the Laser Doppler Velocimeter: Time-Independent Systems," J. Applied Physics, 42, 2, pp. 837-850.

George, W. K. (1971), "An Analysis of the Laser Doppler Velocimeter and Its Application to the Measurement of Turbulence," Ph.D. Thesis, Department of Mechanics, The Johns Hopkins University, Baltimore, Maryland, (Reference I).

George, W. K. and J. L. Lumley (1972), "The Laser Doppler Velocimeter and Its Application to the Measurement of Turbulence," (to be submitted for publication). (Reference II).

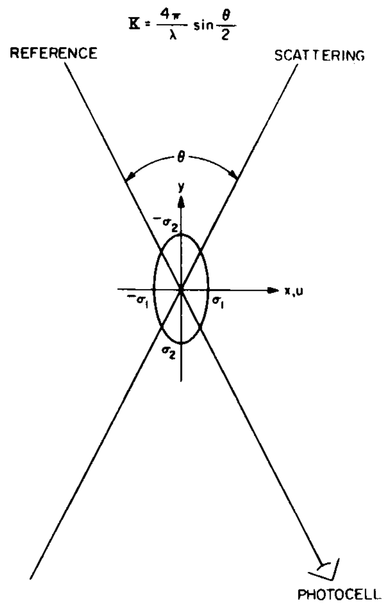

FIGURE 1: SCATTERING VOLUME CROSS SECTION

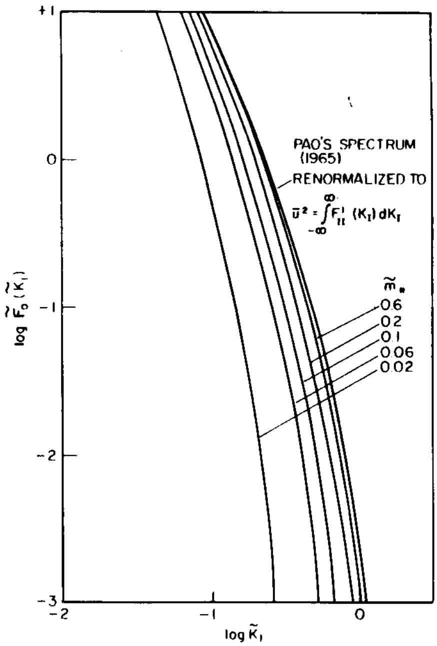

FIGURE 2: SPECTRAL ATTENUATION $\tilde{m}_* = m_* \eta$

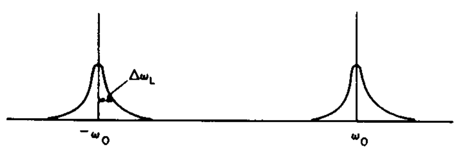

FIGURE 3a: LAMINAR FLOW

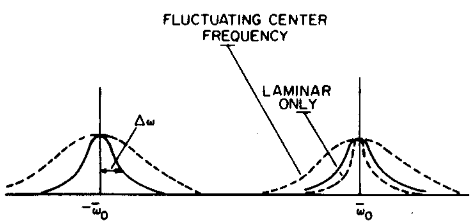

FIGURE 3b: TURBULENT FLOW

SPECTRUM OF THE DOPPLER SIGNAL

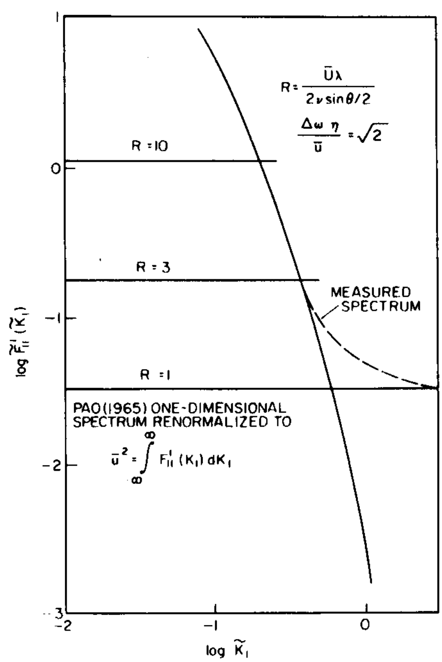

FIGURE 4: AMBIGUITY SPECTRA

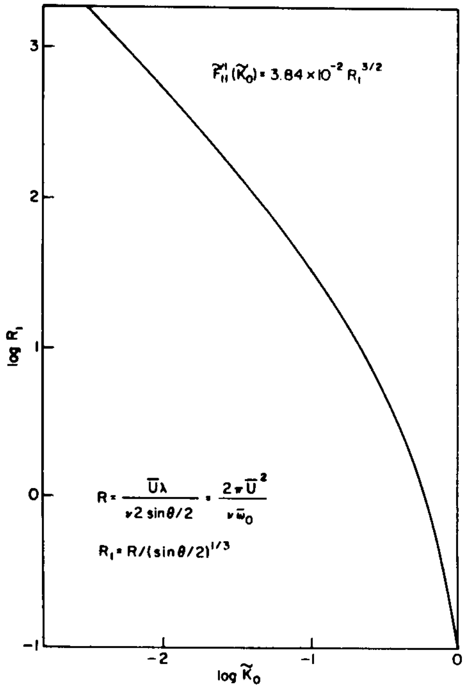

FIGURE 5: VALUE OF R_1 FOR UNITY TURBULENCE/ AMBIGUITY AT INDICATED WAVENUMBER.

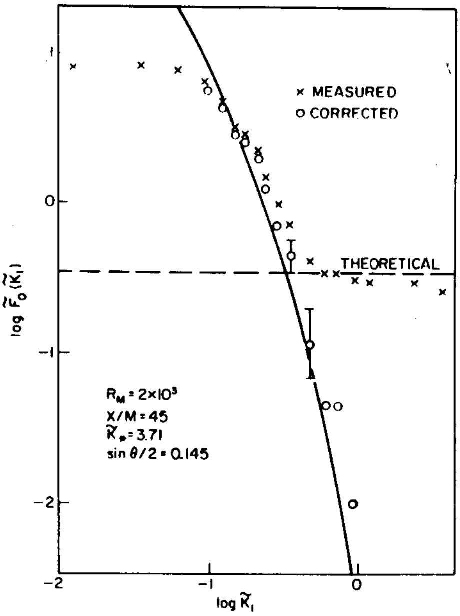

FIGURE 6: COMPARISON OF PREDICTED AND MEASURED SPECTRA IN TURBULENT FLOW.

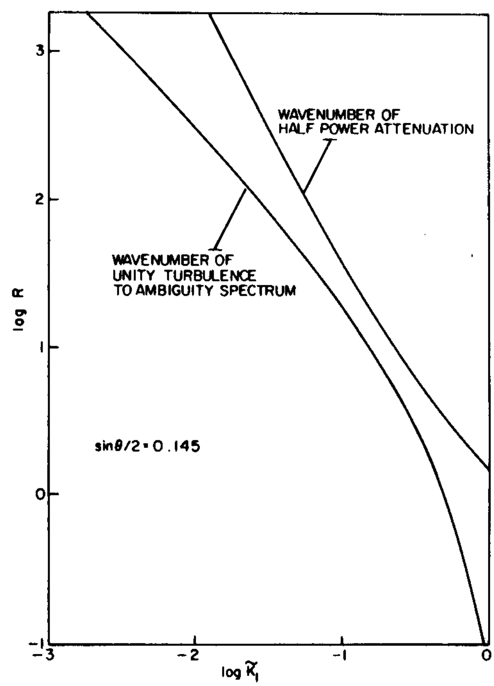

FIGURE 7: COMBINED PLOT OF $R = 2\pi\bar{U}^2/\nu\bar{\omega}_0$ FOR UNITY TURBULENCE/ AMBIGUITY AND HALF POWER ATTENUATION AT INDICATED WAVENUMBERS. SCATTERING VOLUME SELECTED FOR OPTIMUM AMBIGUITY.